© 2020. Published by The Company of Biologists Ltd | Development (2020) 147, dev194019. doi:10.1242/dev.194019

STEM CELLS AND REGENERATION

RESEARCH ARTICLE

Decoding an organ regeneration switch by dissecting cardiac regeneration enhancers

Ian J. Begeman[1,*], Kwangdeok Shin[1,*], Daniel Osorio-Méndez[1], Andrew Kurth[1], Nutishia Lee[2], Trevor J. Chamberlain[3], Francisco J. Pelegri[3] and Junsu Kang[1,4,‡]

ABSTRACT

Heart regeneration in regeneration-competent organisms can be accomplished through the remodeling of gene expression in response to cardiac injury. This dynamic transcriptional response relies on the activities of tissue regeneration enhancer elements (TREEs); however, the mechanisms underlying TREEs are poorly understood. We dissected a cardiac regeneration enhancer in zebrafish to elucidate the mechanisms governing spatiotemporal gene expression during heart regeneration. Cardiac *lepb* regeneration enhancer (*cLEN*) exhibits dynamic, regeneration-dependent activity in the heart. We found that multiple injury-activated regulatory elements are distributed throughout the enhancer region. This analysis also revealed that cardiac regeneration enhancers are not only activated by injury, but surprisingly, they are also actively repressed in the absence of injury. Our data identified a short (22 bp) DNA element containing a key repressive element. Comparative analysis across *Danio* species indicated that the repressive element is conserved in closely related species. The repression mechanism is not operational during embryogenesis and emerges when the heart begins to mature. Incorporating both activation and repression components into the mechanism of tissue regeneration constitutes a new paradigm that might be extrapolated to other regeneration scenarios.

KEY WORDS: Enhancer, Gene expression, Heart, Injury, Regeneration, Zebrafish

INTRODUCTION

Adult mammals permanently lose a substantial number of cardiomyocytes (CMs) after cardiac injury. This limited ability to regenerate lost CMs leads to heart failure and increased morbidity and mortality. By contrast, adult zebrafish possess a remarkable capacity to regenerate damaged hearts (Tzahor and Poss, 2017). In combination with available genetic tools, this ability makes zebrafish a powerful model system for deciphering the mechanisms underlying heart regeneration (Gonzalez-Rosa et al., 2017).

Heart regeneration is a complex process, in which all distinctive components of the cardiac tissue are appropriately coordinated. This elaborate and exquisite event is accomplished by orchestration of both CMs and non-cardiomyocytes. After cardiac injury, non-cardiomyocytes, including those in the epicardium and endocardium, sense injury cues and are rapidly activated to secrete paracrine factors that facilitate heart regeneration (Cao and Poss, 2018; Gonzalez-Rosa et al., 2017). For example, within a day of cardiac injury, the epicardium and endocardium robustly produce retinoic acid, which stimulates CM proliferation (Kikuchi et al., 2011). The endocardium of injured hearts induces *vascular endothelial growth factor Aa* (*vegfaa*), which mediates vasculogenesis, another crucial attribute for heart regeneration (Karra et al., 2018; Marin-Juez et al., 2019). Injury-responsive induction of such factors is required for heart regeneration, and it is crucial that their expression is transient and restricted to the site of injury to ensure proper regeneration. Spatiotemporal induction is important because continuous expression of these factors can have deleterious consequences, such as heart enlargement, cardiac failure and scarring (Gabisonia et al., 2019; Gemberling et al., 2015; Karra et al., 2018; Monroe et al., 2019). However, the mechanism by which spatiotemporal expression of injury-induced factors is achieved during heart regeneration remains a major gap in our knowledge.

Gene transcription in eukaryotes is a complex process that requires specific interactions between transcription factors (TFs) and *cis*-regulatory DNA elements. Among the *cis*-regulatory elements, enhancers are the key to direct spatiotemporal gene expression (Spitz and Furlong, 2012). The activities of enhancers are determined by the binding of TFs to their binding sites, sequence-specific motifs (Shlyueva et al., 2014). Recently, several groups have used regenerative systems, including cardiac tissue, to identify injury-responsive or regeneration-associated enhancers that direct gene expression in injured tissues (Goldman et al., 2017; Harris et al., 2016, 2020; Kang et al., 2016; Lee et al., 2020; Rodriguez and Kang, 2020; Soukup et al., 2019; Suzuki et al., 2019; Thompson et al., 2020; Vizcaya-Molina et al., 2018; Wang et al., 2020, 2019). Comparative analysis combined with transgenic assays in mice identified epicardial enhancers that direct developmental expression, as well as injury-responsive induction in the epicardium (Huang et al., 2012). Unbiased genome-wide analysis revealed multiple tissue regeneration enhancer elements (TREEs) that govern regeneration-dependent gene expression in adult zebrafish and killifish fins and hearts (Goldman et al., 2017; Kang et al., 2016; Thompson et al., 2020; Wang et al., 2020). Although the number of injury/regeneration enhancers, such as TREEs, has expanded, many questions remain regarding the control of their activities and whether multiple mechanisms or a predominant mechanism is responsible for conferring regeneration-induced transcription. Such knowledge is crucial to our understanding of how injury cues are transduced to establish regeneration programs.

Previously, we identified the zebrafish regeneration enhancer linked to *leptin b* (*lepb*) that directs regeneration-specific gene

[1]Department of Cell and Regenerative Biology, School of Medicine and Public Health, University of Wisconsin-Madison, Madison, WI 53705, USA. [2]Department of Cell Biology, Duke University Medical Center, Durham, NC 27710, USA. [3]Laboratory of Genetics, University of Wisconsin-Madison, Madison, WI 53705, USA. [4]UW Carbone Cancer Center, School of Medicine and Public Health, University of Wisconsin-Madison, Madison, WI 53705, USA.
*These authors contributed equally to this work

‡Author for correspondence (junsu.kang@wisc.edu)

J.K., 0000-0001-5286-5426

Handling Editor: Benoit Bruneau
Received 15 June 2020; Accepted 13 November 2020

Development (2020) 147, dev194019. doi:10.1242/dev.194019

expression in the hearts (Kang et al., 2016). Here, we undertake a molecular dissection of *lepb* regeneration enhancer (*LEN*) to decipher how the regulatory elements in regeneration enhancers instruct regeneration-dependent gene expression in the heart. We discovered that a 22 bp DNA segment harbors a repressive sequence and that repression emerges during cardiac maturation. Thus, we propose a new model for regeneration-dependent transcription involving a two-component mechanism; one component mediates injury-responsive activation, and the other component participates in developmental stage-dependent repression. The integration of these components ensures spatiotemporal gene expression during heart regeneration.

RESULTS

Regeneration-dependent expression of cardiac *LEN* (*cLEN*) in endocardial cells

We demonstrated previously that *LEN* is strongly activated during fin and heart regeneration (Kang et al., 2016). To determine the extent of regeneration-specific activation of *LEN*, *LEN* activation was compared in two different injury models: a whole fin amputation model, which causes massive loss of multiple tissues, such as bones, fibroblasts and epidermis, and a fin incision injury model that does not cause tissue loss. A small incision within an inter-ray region induced EGFP signal in *LEN:EGFP*, but the signal intensity was noticeably less robust than that observed after whole fin amputation (Fig. S1B). These results indicate that *LEN* is activated by injury and is a TREE.

Our previous study demonstrated that *LEN* contains two tissue-specific modules that function independently in the fin and heart (Kang et al., 2016). The fin *LEN* regeneration module (*fLEN*) is located in the central portion of *LEN*, whereas the cardiac *LEN* regeneration module (*cLEN*) is located proximally, in nucleotides 1034-1350 of *LEN* (Fig. 1A). Although injury-responsive activity of *cLEN* was examined using adult hearts in a previous study (Kang et al., 2016), the activity of the 317 bp *cLEN* fragment has not been studied during heart development and regeneration.

To determine the regeneration-dependent activity of *cLEN*, EGFP expression was determined in *cLEN:EGFP* reporter fish, which carry *cLEN* coupled to the *lepb* 2 kb minimal promoter (*P2*) and *EGFP* cassette, in uninjured and regenerating hearts during development. *cLEN:EGFP* fish were crossed with the *cardiac myosin light chain 2* (*cmlc2*):*mCherry-nitroreductase* (*NTR*) strain, which enables genetic

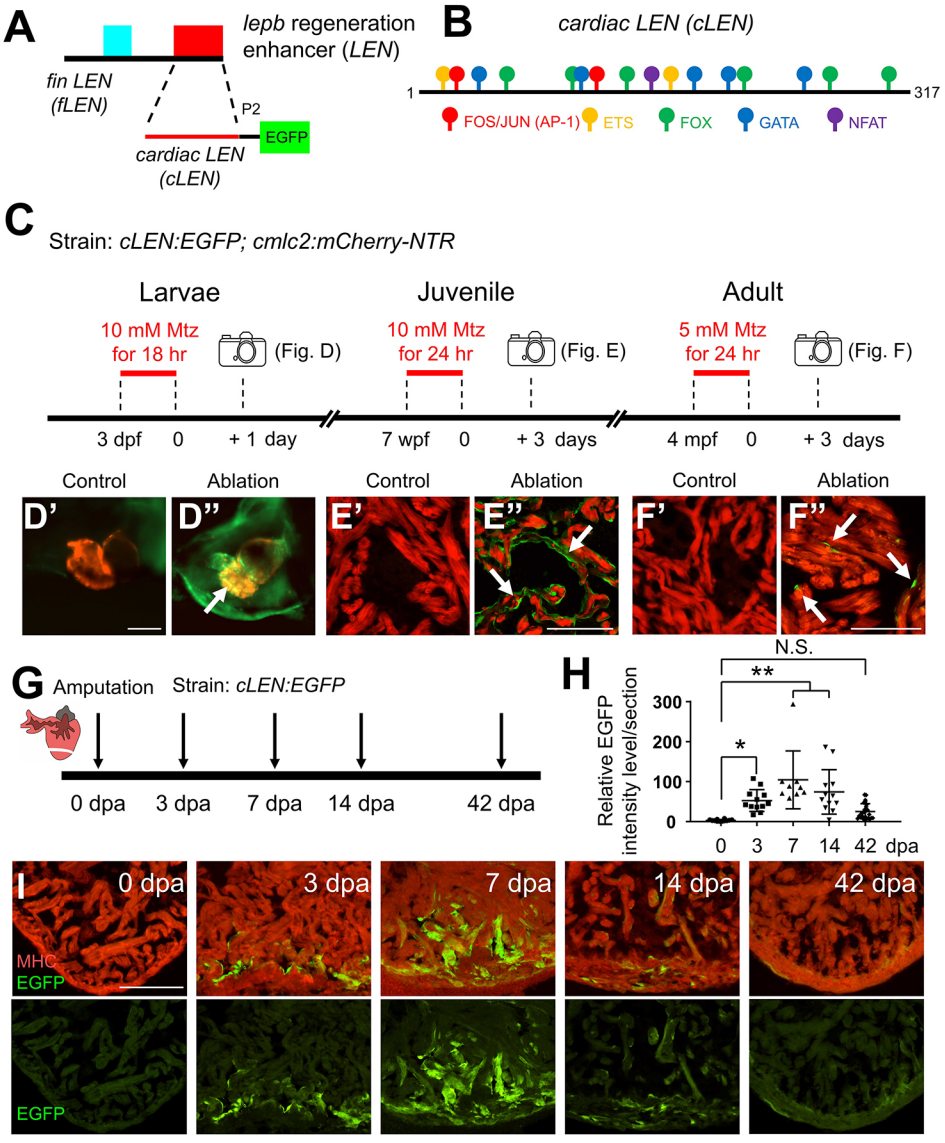

Fig. 1. Regeneration-dependent activity of cardiac *LEN* (*cLEN*). (A) Schematic of *lepb* regeneration enhancer (*LEN*) containing two tissue-specific regeneration modules. A transgene construct examined for *cLEN* activity consists of 317 bp of *cLEN*, *lepb* 2 kb upstream promoter (*P2*) and *EGFP* reporter sequences. (B) Schematic of *cLEN* annotated with predicted TF binding sites. (C-F) Zebrafish strain and experimental strategy undertaken to ablate CMs (C) and images of uninjured and ablated hearts in larvae (D), juveniles (E) and adults (F). (G-I) Dynamic *cLEN* activity during zebrafish heart regeneration. (G) Experimental design to determine *cLEN* activity during heart regeneration. (H) Quantification of EGFP expression intensity normalized to images of wild-type uninjured hearts at the wound area. The data are presented as the mean±s.d. Numbers of animals are shown in Table S3. **P*<0.05; ***P*<0.01; N.S., not significant. One-way ANOVA with Tukey's post-hoc test. (I) Images of cardiac sections of uninjured and regenerating hearts. Scale bars: 100 µm in E″, F″,I; 50 µm in D′.

Development (2020) 147, dev194019. doi:10.1242/dev.194019

ablation of CMs (Chen et al., 2013; Curado et al., 2007). In this strain, the bacterial *NTR* gene is controlled by the *cmlc2* regulatory element (Rottbauer et al., 2002), resulting in CM-specific NTR expression. The innocuous prodrug metronidazole (Mtz) is converted into a cytotoxic molecule by NTR in CMs of *cmlc2:mCherry-NTR* fish, thereby ablating a significant number of CMs. *cLEN* activity was examined in uninjured and injured hearts at 5 days post-fertilization (dpf), 7 weeks post-fertilization (wpf) and 4 months post-fertilization (mpf), representing larval, juvenile and adult stages, respectively. This assay demonstrated that EGFP is undetectable in uninjured hearts but is strongly induced upon ablation at all three stages (Fig. 1C-F), indicating that *cLEN* is not a developmental enhancer in the hearts and that injury signals are required for its activity. Cardiac ablation in larvae results in a pericardial edema phenotype, potentially inducing a systemic injury response owing to insufficient circulation and subsequently activating *cLEN* in the epidermis (Fig. S2A). By contrast, cardiac ablation in adults did not direct ectopic expression in the epidermis (Fig. S2A). Epidermal induction upon local injury was not observed in amputated adult caudal fins, suggesting that ectopic *cLEN* activation in the epidermis is repressed in adults (Fig. S1C). Mtz treatment did not induce EGFP in the absence of *cmlc2:mCherry-NTR*, confirming the specificity of cardiac injury-responsive activation of *cLEN* (Fig. S2B).

To explore *cLEN* activity further during adult heart regeneration, *cLEN:EGFP* expression was quantified throughout heart regeneration in adult fish. Ventricular apices of *cLEN:EGFP* fish were amputated, and hearts were collected at 3, 7, 14 and 42 days post-amputation (dpa), in addition to uninjured hearts (Fig. 1G). EGFP expression was examined by immunostaining cardiac sections with antibodies against EGFP, myosin heavy chain (MHC), a CM marker, and Raldh2, an endocardial and epicardial marker. EGFP was undetectable in uninjured hearts but was strongly induced at 3 dpa, mainly in endocardial cells, indicating that cardiac injury activates *cLEN* (Fig. 1H,I; Fig. S3A). EGFP intensity peaked at 7 dpa and remained high at 14 dpa, suggesting that *cLEN* activity was maintained during heart regeneration (Fig. 1H,I). However, EGFP expression was barely detectable at 42 dpa, when heart regeneration was completed (Fig. 1H,I). This dynamic *cLEN* activity during regeneration demonstrates that *cLEN* is a cardiac TREE.

Multiple sequences mediating activation are distributed throughout *cLEN*

Enhancer activity is determined by the binding of transcription-promoting TFs to their binding sites (Spitz and Furlong, 2012). Cardiac injury-responsive activation motifs are poorly characterized owing to the low number of regeneration enhancer studies (Rodriguez and Kang, 2020; Soukup et al., 2019); hence, we focused on motifs representing tissues or cells displaying enhancer activity. *cLEN* is active in the endocardium, the innermost layer of endothelial cells in the heart (Fig. S3A). Motif analysis of *cLEN* using JASPAR, a database of TF binding profiles (Khan et al., 2018), and searching for consensus binding sequence information revealed that *cLEN* contains predicted binding sites for TFs associated with endothelial/endocardial cells, such as nuclear factor of activated T-cells (NFAT), GATA, Forkhead (FOX) and ETS (De Val and Black, 2009; De Val et al., 2008; Meadows et al., 2011; Nemer and Nemer, 2002; Norrmén et al., 2009; Park et al., 2013; Zhou et al., 2005). There is one NFAT, five GATA, six FOX and two ETS sites within *cLEN* (Fig. 1B; Fig. S4).

In silico motif analysis predicts potential TF binding sites, but we probed the activity of potential *cis*-regulatory elements using transgenic enhancer assays (Kvon, 2015). An enhancer reporter system with various *cLEN* fragments was used to identify the essential *cis*-regulatory elements in *cLEN* that mediate injury-responsive gene activation. Initially, *cLEN* was fragmented into two parts: 144 bp of distal *cLEN(1-144)*, named *cLEN-dis*, and 177 bp of proximal *cLEN(141-317)*, named *cLEN-pro*. Transgenic reporter lines carrying *cLEN-dis* or *cLEN-pro* were unable to direct endocardial EGFP expression in 3 dpa hearts, indicating that these fragments are not sufficient for injury-responsive expression in the endocardium (Fig. 2A,B; Fig. S5).

Notably, *cLEN(131-164)* overlaps parts of *cLEN-dis* and *cLEN-pro* and contains binding motifs for FOX, NFAT and ETS within a single 34 bp region (Fig. S4), leading us to examine whether the FOX-NFAT-ETS (FNE) motifs are essential for endocardial expression. We generated a new transgenic line carrying a small (54 bp) fragment of *cLEN(118-171)*, named *cLEN-FNE*, and examined their activity in hearts (Fig. 2A). Similar to *cLEN-dis* and *cLEN-pro*, *cLEN-FNE* was unable to direct endocardial EGFP expression in 3 dpa hearts, demonstrating that the FNE motifs in *cLEN* are not sufficient to drive regeneration-dependent endocardial expression (Fig. 2B; Fig. S5). Given that *cLEN-dis*, *cLEN-pro* and *cLEN-FNE* cover the full sequence of *cLEN*, these results suggest that at least two regulatory elements located in *cLEN-dis* and *cLEN-pro* are required for regeneration-dependent activation.

Activator protein 1 (AP-1) is a well-characterized injury-responsive factor in various contexts, including Schwann cells, fins and the heart (Alfonso-Jaume et al., 2006; Beisaw et al., 2020; Hung et al., 2015; Ishida et al., 2010; Shirali et al., 2018; Yates and Rayner, 2002), and *cLEN* contains two AP-1 sites (Fig. S4). A recent study also demonstrated that GATA and ETS motifs are crucial components of regeneration enhancers (Soukup et al., 2019). Thus, the involvement of AP-1, GATA and FNE motifs in regeneration enhancer activity was tested. The results indicated that *cLEN(107-238)*, named *cLEN-act*, which contains AP-1, GATA and FNE motifs, was able to drive regeneration-dependent endocardial expression (Fig. 2B; Fig. S5). Developmental enhancers are known to be regulated by multiple regulatory elements (Spitz and Furlong, 2012); hence, these results indicate that cardiac regeneration enhancers are also regulated by multiple *cis*-regulatory elements.

To test the involvement of the AP-1 binding sites in injury-responsive activation, two AP-1 motifs in *cLEN* were mutated to generate $cLEN^{AP\text{-}1m}$, and their activity was examined in the F_0 mosaic injured hearts. Several constructs were generated, including *P2:EGFP* (minimal promoter, negative control), *cLEN:EGFP* (positive control) and $cLEN^{AP\text{-}1m}$*:EGFP* (Fig. 2C). These constructs were injected into the one-cell stage of *cmlc2:mCherry-NTR* embryos, and EGFP expression was examined before and after cardiac ablation (Fig. 2D). None of these constructs was able to direct EGFP expression in uninjured hearts. Upon cardiac injury, a significant number of larvae carrying the intact *cLEN* directed EGFP induction (Fig. 2E). However, the majority of larvae with *P2* or $cLEN^{AP\text{-}1m}$ were not able to direct injury-responsive expression (Fig. 2E), indicating that AP-1 binding sites are required for injury-responsive activity.

We next attempted to build a synthetic version of a cardiac regeneration enhancer by combining TF binding sites present in *cLEN-act*. Three copies of AP-1-FOX-NFAT-ETS-GATA sites were coupled with the *P2* minimal promoter and *EGFP* sequences to produce *AFNEGx3*, and its activity was examined in the F_0 mosaic injured hearts. EGFP was undetectable in 3 dpf uninjured hearts. Noticeable EGFP induction was detected in some mosaic injured hearts carrying *AFNEGx3* (Fig. S6D); however, the majority of larvae did not demonstrate injury-responsive EGFP induction (Fig. 2E). These data suggest that further dissection of *cLEN* is

Development (2020) 147, dev194019. doi:10.1242/dev.194019

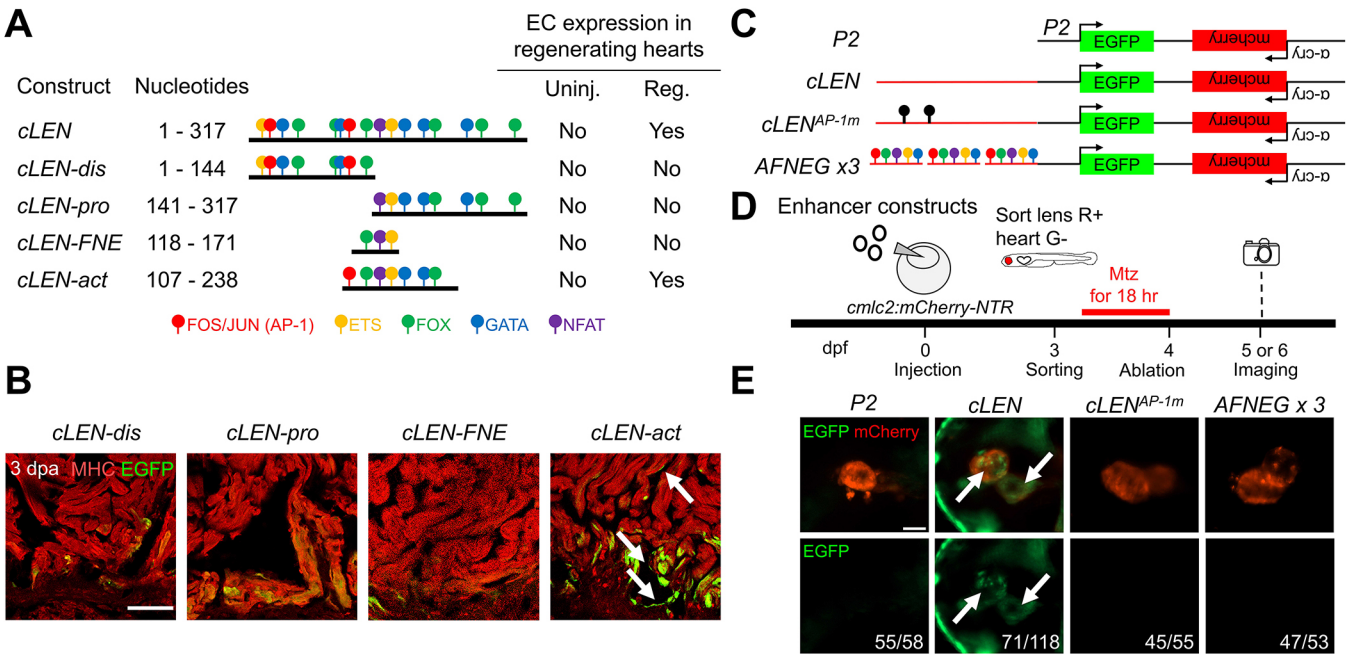

Fig. 2. Molecular dissection of *cLEN* to identify the fragment containing injury-responsive elements. (A) Transgene constructs examined for regeneration-dependent expression in response to cardiac injury. Endocardial expression results are summarized on the right. EC, endocardial cell. Uninj. and Reg. correspond to uninjured and 3 dpa regenerating hearts, respectively. (B) Images of sections of 3 dpa hearts from transgenic fish carrying *cLEN* fragments. Numbers of animals are shown in Table S3. The arrows indicate endocardial EGFP induction. Note that the *P2* promoter directs basal expression in CMs in response to injury (see Fig. S3; Kang et al., 2016). MHC, myosin heavy chain, a CM marker. (C) Transgenic constructs used to examine enhancer activity in the F_0 mosaic injured hearts. Two AP-1 binding sites were mutated in *cLEN*$^{AP\text{-}1m}$ (black circles). *AFNEGx3* is a synthetic cardiac regeneration enhancer consisting of three tandem copies of the AP-1-FOX-NFAT-ETS-GATA motifs. (D) Schematic of enhancer assays in the F_0 mosaic hearts. (E) Images of injured hearts of larvae injected with *P2*, *cLEN*, *cLEN*$^{AP\text{-}1m}$ and *AFNEGx3*. Note that larvae carrying transgenic constructs were selected by mCherry expression in the lens, without a cardiac EGFP signal. The arrows indicate injury-responsive EGFP induction in the injured hearts. Numbers at the bottom corners indicate the total ratio of embryos showing the corresponding expression pattern. Scale bars: 100 µm in B; 50 µm in E.

required to create a functional synthetic regeneration enhancer. In addition, enhancer assays with stable lines will be required to deduce the activity of *AFNEGx3*.

A recent study demonstrated that co-injection of mRNAs of the AP-1 complex components, *junba* and *fosl1a*, into one-cell-stage embryos is sufficient to activate the expression of AP-1 target genes (Beisaw et al., 2020). To determine whether AP-1 TFs can activate *cLEN*, *mCherry*, AP-1 (*junba/fosl1a*), *nfatc1* or *nfatc1*+AP-1 mRNAs were injected into the one-cell stage of *cLEN:EGFP* heterozygote embryos, and EGFP expression was assayed at 1 day (Fig. S6A). Although *mCherry* or *nfatc1* mRNA injection was unable to induce EGFP, we observed that a significant number of embryos injected with AP-1 or *nfatc1*+AP-1 demonstrated EGFP expression (Fig. S6C), suggesting that AP-1 contributes to the activation of *cLEN*. Overall, our data suggest that AP-1 is an important injury-activating factor for *cLEN*.

A repressive mechanism ensures spatiotemporal gene expression in the heart

Although our data suggest that FNE motifs are not sufficient for regeneration-dependent activation, it is unclear whether FNE motifs are necessary. To examine this, we generated another transgenic line, which carries *cLEN* without a 47 bp sequence harboring the FNE motifs: *cLEN(1-317Δ122-168)*, referred to as *cLENΔ47* (Fig. 3A). Unexpectedly, although *cLEN* was inactive, *cLENΔ47* exerted ectopic activity in the uninjured hearts (Fig. 3B; Fig. S7). Three independent lines of *cLENΔ47* demonstrated endocardial EGFP expression in uninjured hearts. Although EGFP was undetectable in uninjured hearts of *cLEN* lines (0.001 and 0.016 µm^2/100 µm^2 in line 3 and 7, respectively), EGFP was expressed in *cLENΔ47* uninjured hearts (0.912 and 1.04 µm^2/100 µm^2 in line 3 and 6, respectively) (Fig. 3C). This ectopic expression pattern suggests the presence of an inhibitory element in the deleted 47 bp sequence (*cLEN-47*).

Next, we explored how repression is lifted upon cardiac injury. To this end, we examined the EGFP expression patterns of *cLEN* and *cLENΔ47* in regenerating hearts. In 3 dpa hearts, both *cLEN* and *cLENΔ47* directed EGFP expression in the border zone (5.66, 10.95, 12.99 and 15.62 µm^2/100 µm^2 in *cLEN* line 3 and 7 and *cLENΔ47* line 3 and 6, respectively), demonstrating their activation abilities in response to injury (Fig. 3B,D). The EGFP$^+$ cells were colocalized with Raldh2$^+$ cells, indicating that *cLEN* and *cLENΔ47* were active mainly in the endocardial cells at the wound (Fig. S3A). By contrast, *cLEN* and *cLENΔ47* displayed distinct enhancer activities in the region distant from the wound area (the remote zone). Although the EGFP$^+$ area was very limited in the remote zone of *cLEN* (0.35 and 0.55 µm^2/100 µm^2 in line 3 and 7, respectively), regenerating *cLENΔ47* hearts demonstrated EGFP expression in a significant endocardial area of the remote zone (4.94 and 5.43 µm^2/100 µm^2 in line 3 and 6, respectively) (Fig. 3E; Fig S3A,B; Fig. S8A-C). These results indicate that the inhibitory element in *cLEN-47* is deactivated in the border zone but remains functional in the remote zone. *cLEN* activity returned to a level similar to that in the uninjured hearts at 42 dpa (Fig. 1H,I; Fig. S8D); however, significant EGFP expression was detected in the *cLENΔ47* hearts at 42 dpa (Fig. S8D,E), suggesting that the repressive elements are functional and restrict TREE activity after the completion of regeneration. Our results provide evidence that cardiac regeneration enhancers are actively repressed in uninjured and regenerating

Development (2020) 147, dev194019. doi:10.1242/dev.194019

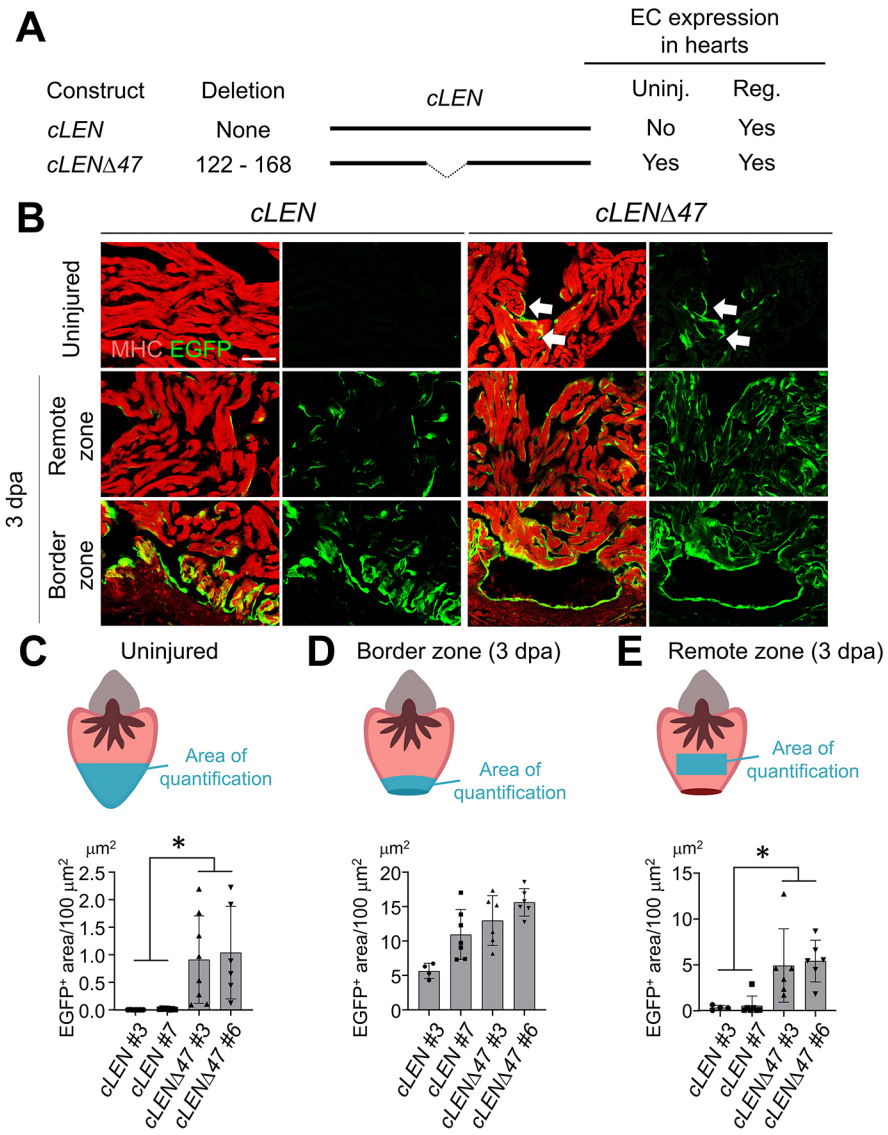

Fig. 3. Active repression of *cLEN* establishes spatiotemporal gene expression in uninjured and regenerating hearts. (A) Transgene constructs examined for reporter gene expression. Endocardial expression results are summarized on the right. EC, endocardial cell. Uninj. and Reg. correspond to uninjured and 3 dpa regenerating hearts, respectively. (B) Images of sections of transgenic fish carrying *cLEN* and *cLENΔ47*. Top, uninjured hearts. Middle, remote zone of 3 dpa hearts. Bottom, border zone of 3 dpa hearts. The arrows indicate endocardial EGFP expression. (C-E) Top, schematic of uninjured and 3 dpa hearts. Area of quantification is marked in blue. Bottom, quantification of EGFP$^+$ area per 100 µm^2 cardiac tissue in uninjured hearts (C), border zone (D) and remote zone (E) of 3 dpa hearts. Data are presented as the mean±s.d. Numbers of animals are shown in Table S3. *P<0.05, one-way ANOVA with Tukey's post-hoc test. Scale bar: 100 µm in B.

hearts to prevent aberrant gene expression, revealing intricate modulation of regeneration enhancers in the heart.

A 22 bp sequence in *cLEN* suppresses regeneration enhancer activity

To exclude the possibility that the 47 bp deletion places two activation elements close to each other or creates a *de novo* activation element, thereby aberrantly stimulating regeneration enhancers in the absence of injury, we created a series of five new 11 bp deletion lines, named *cLENΔ11-1* to *cLENΔ11-5*, which together covered the deleted *cLEN-47* fragment (Fig. 4A). Notably, our analyses with uninjured hearts demonstrated that *cLENΔ11-1* and *-2*, but not *cLENΔ11-3* to *-5*, drive ectopic endocardial expression in uninjured hearts (Fig. 4B). The EGFP$^+$ cardiac tissues were 3.28 and 1.04 µm^2/100 µm^2 in uninjured hearts of *cLENΔ11-1* and *-2*, respectively. By contrast, EGFP expression was limited in uninjured hearts of *cLENΔ11-3*, *-4*, and *-5* (0.03, 0.08 and 0.01 µm^2/100 µm^2, respectively; Fig. 4C). In 3 dpa regenerating adult hearts, all five constructs were capable of directing injury-responsive gene expression in the border zone (16.77, 15.86, 20.98, 5.12 and 6.96 µm^2/100 µm^2 for *cLENΔ11-1* to *-5*, respectively; Fig. 4B,D), indicating that injury-responsive activity is intact regardless of these 11 bp deletions. *cLENΔ11-4* and *-5* had smaller areas of EGFP-expressing cells, compared with those in other *cLENΔ11* lines, suggesting that deletion of the potential activation motifs, such as ETS, may influence injury-responsive activity in the border zone. In the remote zone, EGFP expression was limited in *cLENΔ11-3* (0.69 µm^2/100 µm^2) and was barely detectable in *cLENΔ11-4* and *-5*, (0.10 and 0.29 µm^2/100 µm^2 for *cLENΔ11-4* and *-5*, respectively), highlighting regional activation of the cardiac regeneration enhancer in the border zone. Although the EGFP$^+$ area was larger in *cLENΔ11-1* versus *cLENΔ11-2* (3.96 versus 1.24 µm^2/100 µm^2, respectively), a significant number of endocardial cells in the remote zone expressed EGFP in *cLENΔ11-1* and *cLENΔ11-2* (Fig. 4E). Similar to *cLENΔ47*, *cLENΔ11-1* and *-2* exhibited significant GFP expression at 42 dpa (Fig. S8D). These results confirm that ectopic activation is caused by deletion of a repressive element rather than altered spacing of chromatin structure. This repressive element resides within the 22 bp region of *cLEN(121-142)* or *cLEN-22*.

Comparative analysis of *cLEN* across teleost species identifies an important repressive element in *cLEN*

To identify an essential repressive element in *cLEN*, we explored orthologous *cLEN* regions in other fish species. Similar to zebrafish,

Development (2020) 147, dev194019. doi:10.1242/dev.194019

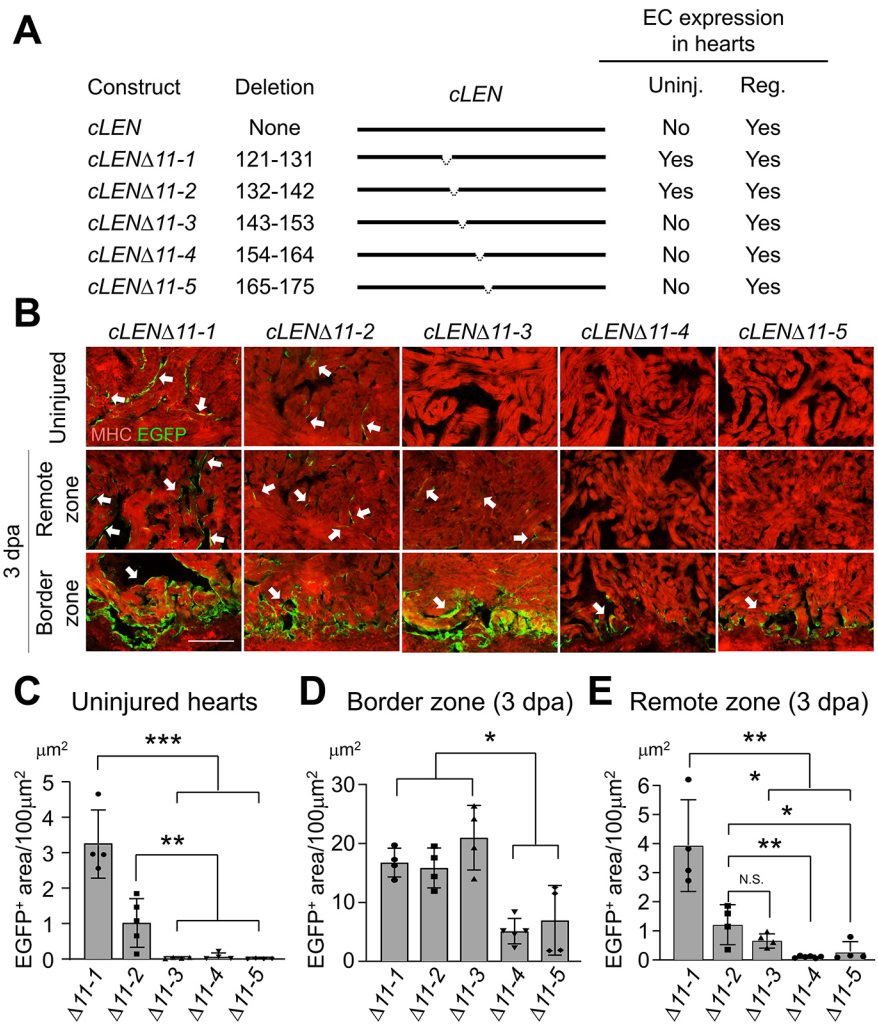

Fig. 4. Evidence of the presence of a repressive element within a 22 bp *cLEN* sequence. (A) Transgene constructs examined for reporter gene expression. Endocardial expression results are summarized on the right. EC, endocardial cell. Uninj. and Reg. correspond to uninjured and 3 dpa regenerating hearts, respectively. (B) Images of sections of transgenic fish carrying *cLEN* deletion transgenes. Top, uninjured hearts. Middle, the remote zone of 3 dpa hearts. Bottom, the border zone of 3 dpa hearts. The arrows indicate endocardial EGFP expression. (C) Quantification of EGFP$^+$ area per 100 μm^2 cardiac tissue in uninjured hearts. (D) Quantification of EGFP$^+$ area per 100 μm^2 cardiac tissue in the border zone of 3 dpa hearts. (E) Quantification of EGFP$^+$ area per 100 μm^2 cardiac tissue in the remote zone of 3 dpa hearts. The data are presented as the mean±s.d. Numbers of animals are shown in Table S3. *P<0.05; **P<0.01; ***P<0.001; N.S., not significant. One-way ANOVA with Tukey's post-hoc test. Scale bar: 100 μm in B.

the genomes of 15 other teleost fish models contain multiple *leptin* genes. These species include the golden-line barbel (*Sinocyclocheilus grahami*), horned golden-line barbel (*Sinocyclocheilus rhinocerous*), blind barbel (*Sinocyclocheilus anshuiensis*), common carp (*Cyprinus carpio*), goldfish (*Carassius auratus*), Mexican tetra (*Astyanax mexicanus*), red-bellied piranha (*Pygocentrus nattereri*), electric eel (*Electrophorus electricus*), Atlantic herring (*Clupea harengus*), denticle herring (*Denticeps clupeoides*) and Japanese medaka (*Oryzias latipes*). Zebrafish, Mexican tetra, red-bellied piranha, electric eel, Atlantic herring, denticle herring, and Japanese medaka possess two *leptin* paralogs: *lepa* and *lepb* (Gorissen et al., 2009). The lineage containing the barbel, carp and goldfish species underwent an additional round of genome duplication, resulting in four *leptin* genes: *lepa1*, *lepa2*, *lepb1* and *lepb2* (Gorissen and Flik, 2014; Huising et al., 2006). Using reference genomes from the Ensembl database, *lepb* upstream sequences from these fish species were compared with the zebrafish sequence via limited area global alignment of nucleotides (LAGAN) analysis (Brudno et al., 2007). This sequence comparison detected limited conservation or lack of conservation of *cLEN* upstream of *lepb* across these species (Fig. S9A,B). However, manual comparison revealed that *cLEN-act* is moderately conserved in zebrafish, barbel, carp and goldfish, all of which belong to the Cyprinidae family. An AP-1 binding site within *cLEN-act* appears to be conserved across the Cyprinidae species, whereas *cLEN-22* containing a repressive element displays sequence diversity (Fig. S9C).

Owing to limited or undetectable conservation of *cLEN* in other teleost species, *cLEN* conservation was assessed in closely related species. Orthologous *cLEN* was evaluated within the *Danio* genus, to which *Danio rerio* (zebrafish) belongs. To compare the sequence, we extracted genomic DNA and isolated the *cLEN* equivalent fragments from *Danio aesculapii*, *Danio kyathit* and *Danio albolineatus*. Sequencing of *cLEN* identified that the AP-1 motif is present in the *cLEN-act* region (Fig. S9C). RT-qPCR or RT-PCR analysis in *D. aesculapii* and *D. kyathit* demonstrated that *lepb* is induced in response to cardiac injury, suggesting that the injury-responsive activity of *cLEN* is conserved in other *Danio* species (Fig. 5D,E). We next aimed to identify the repressive element in *cLEN* by comparison of *cLEN-22*. Intriguingly, counterparts of *cLEN-22* displayed 6 or 9 bp DNA insertions (Fig. 5A). This observation raises a question of whether the functionality of the repressive element might be disrupted by these insertions. To assess the activity of *cLEN-22* variants from other *Danio* species, a 6 bp insertion was introduced into the zebrafish *cLEN* to generate *cLEN*^{ins6bp}*:EGFP* transgenic fish. Two independent lines of *cLEN*^{ins6bp}*:EGFP* were able to induce EGFP expression in response to cardiac injury, indicating that a 6 bp insertion does not affect injury-responsive *cLEN* function (Fig. 5B). Unlike *cLENΔ47*, *cLENΔ11-1* and *cLENΔ11-2*, *cLEN*^{ins6bp}*:EGFP* transgenic fish were unable to direct ectopic endocardial expression in uninjured hearts (Fig. 5B), and *lepb* transcript levels were not significantly increased in uninjured hearts of other *Danio*

Development (2020) 147, dev194019. doi:10.1242/dev.194019

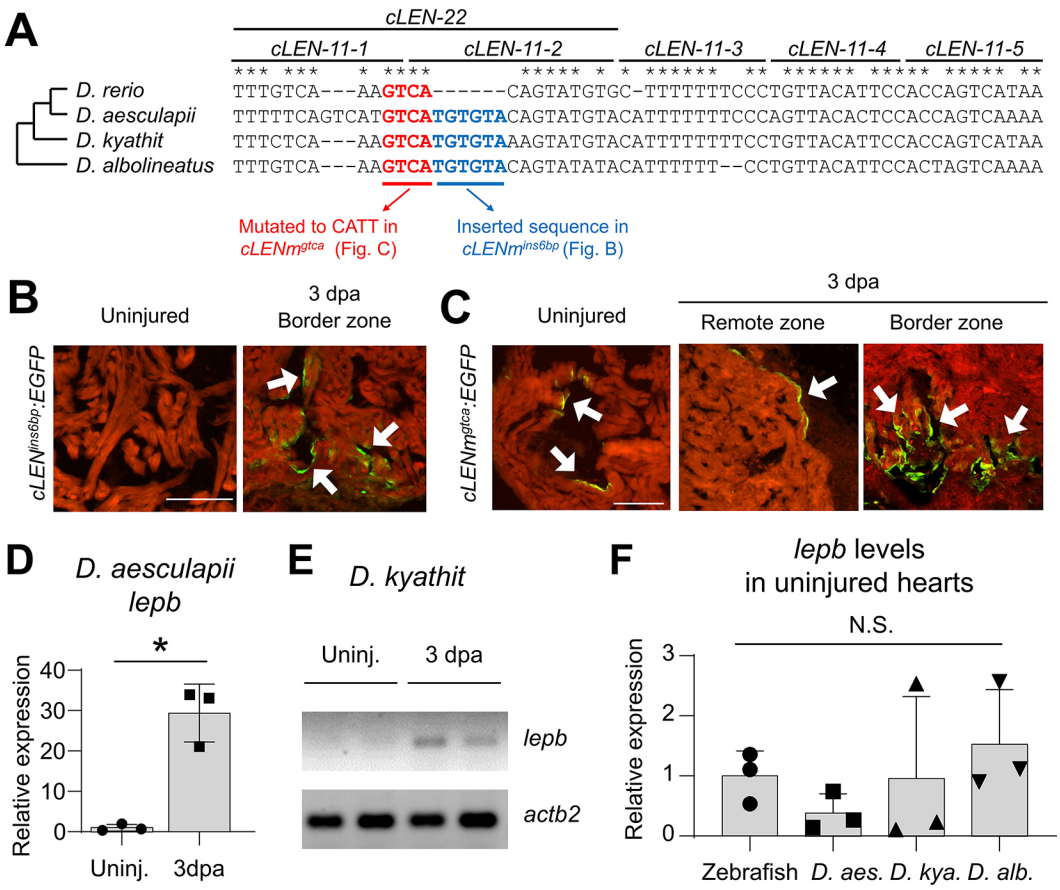

Fig. 5. The *cLEN* repressive element, but not a neighboring sequence, is present in other *Danio* species. (A) Alignment of orthologous sequences of *cLEN11-1* to *cLEN11-5* in *Danio* species, including *Danio rerio*, *Danio aesculapii*, *Danio kyathit* and *Danio albolineatus*. *cLEN-22* contains 6 or 9 bp insertions in non-zebrafish sequences. Asterisks indicate conserved base pairs. The conserved GTCA sequence overlapping *cLEN-11-1* and *cLEN-11-2* is marked in red. Dendrogram indicates phylogenetic relationship. (B) Images of cardiac sections of *cLEN^{ins6bp}:EGFP* transgenic fish harboring a 6 bp insertion (TGTGTA). (C) Images of cardiac sections of *cLENm^{gtca}:EGFP* transgenic fish harboring the mutation of GTCA to CATT. The arrows indicate endocardial EGFP expression. Numbers of animals are shown in Table S3. (D) RT-qPCR analysis of *lepb* in uninjured and 3 dpa hearts of *D. aesculapii*. (E) RT-PCR of samples from the uninjured and 3 dpa hearts of *D. kyathit*. *actb2* was used as the loading control. Uninj., uninjured hearts. (F) RT-qPCR analysis of *lepb* in the uninjured hearts of zebrafish, *D. aesculapii*, *D. kyathit* and *D. albolineatus*. The data are presented as mean±s.d., *n*=3; *lepb* transcript levels were normalized to *actb2* levels in D,F. **P*<0.05; N.S., not significant. Student's unpaired, two-tailed *t*-test. Scale bars: 100 µm in B,C.

species (Fig. 5F). These results demonstrate that this 6 bp insertion does not interfere with the function of the repressive element.

Given that deletion of either *cLEN11-1* or *cLEN11-2* impedes repression, we focused on a sequence spanning these two fragments. The juxtaposition of *cLEN11-1* and *cLEN11-2* has a GT/CA sequence that is conserved in other *Danio* species and some barbel, carp and goldfish *lepb* paralogs (Fig. 5A; Fig. S9C). Our motif analysis of *cLEN-22* using the JASPAR database predicted binding sites for two repressors: *growth factor independent 1B transcription repressor* (*gfi1b*) and *PR domain containing 1a, with ZNF domain* (*prdm1a*). *gfi1b* is the key repressor controlling hematopoiesis (Dahl et al., 2007; Li et al., 2010; Saleque et al., 2007). *prdm1a* acts as a repressor in the intestine and immune cells (Harper et al., 2011; Hohenauer and Moore, 2012; Kallies et al., 2006; Muncan et al., 2011). To test whether their binding sites are responsible for the repression, the JASPAR database was used to design a mutation that disrupts the Prdm1a and Gfi1b binding sites and is not predicted to create new binding sites or disturb spacing between other candidate sites. Based on this analysis, the GTCA sequence was mutated to CATT. To test whether the GTCA sequence comprises the crucial repressive motif, new transgenic fish with the GTCA to CATT mutation were generated, named *cLENm^{gtca}*. In 3 dpa hearts, two independent lines of *cLENm^{gtca}:EGFP* were able to drive injury-responsive expression in the border zone (Fig. 5C). By contrast, endocardial EGFP expression was limited in the remote zone of 3 dpa hearts (Fig. 5C). We next examined EGFP expression in uninjured hearts. Interestingly, *cLENm^{gtca}* directed ectopic EGFP expression in some endocardial cells in uninjured hearts (Fig. 5C). Although the GTCA mutation does not completely recapitulate the activity of *cLEN* deletion constructs in uninjured hearts, these results indicate that GTCA is a part of an essential repressive element in *cLEN*.

Repression emerges during cardiac maturation

During development, the heart matures to form highly organized sarcomere structures (Fukuda et al., 2019; Huang et al., 2009). To determine when repression begins to function, EGFP expression in the *cLEN* and *cLENΔ47* reporter lines was evaluated. First, we confirmed that CM ablation injuries drive EGFP induction in the *cLEN*, *cLENΔ47* and *cLENΔ11-1* to *-5* reporter lines at the 5 dpf larval stage, indicating that activation elements respond to injury from early developmental stages (Fig. S10).

To examine when the repression mechanism begins to be operational during development, cardiac section samples were

Development (2020) 147, dev194019. doi:10.1242/dev.194019

collected from *cLEN:EGFP;cmlc2:mCherry* and *cLENΔ47:EGFP;cmlc2:mCherry* at 5, 10, 14 and 35 dpf, and EGFP signals were amplified by immunostaining. EGFP was undetectable in 5 dpf hearts of *cLEN* and *cLENΔ47* (n=17 and 13 for *cLEN* and *cLENΔ47*, respectively). Although EGFP expression was not observed in the *cLEN* hearts at later time points (n=17 and 20 at 10 and 14 dpf, respectively), EGFP in the *cLENΔ47* hearts was visible at 10 dpf in 12 of 12 examined hearts and at 14 dpf in 14 of 14 examined hearts. At 35 dpf, uninjured hearts of all *cLENΔ47* animals showed EGFP signals (n=6) (Fig. 6). A recent study demonstrated that trabecular CMs undergo significant morphological changes, including an increase in myofilament thickness, by 5 dpf, representing cardiac maturation (Fukuda et al., 2019). Given that *cLENΔ47* becomes active in uninjured hearts after 5 dpf, our data indicate that repression is not operational in uninjured hearts during embryogenesis but emerges during cardiac maturation.

DISCUSSION

Tissue regeneration is accomplished by dynamic changes in gene transcription. Recently, multiple studies have demonstrated that regeneration-dependent or injury-responsive gene expression relies on the activities of enhancers, such as TREEs (Goldman et al., 2017; Harris et al., 2020; Huang et al., 2012; Kang et al., 2016; Lee et al., 2020; Rodriguez and Kang, 2020; Thompson et al., 2020; Vizcaya-Molina et al., 2018; Wang et al., 2020); yet underlying enhancer mechanisms have remained elusive. In the present study, we carried out a molecular dissection of the cardiac regeneration enhancer *cLEN* in zebrafish to elucidate mechanisms controlling regeneration enhancer activity. Regeneration-dependent activity of *cLEN* is detected mainly in the endocardium, which is the first cardiac tissue that responds to injury. An interesting feature of regenerative events in the endocardium is rapid organ-wide regenerative factor induction. This organ-wide gene activation is promptly restricted to the wound area within a day, and this restriction might be necessary to prevent ectopic regeneration outcomes in the remote zone, a region distant from the wound area where regeneration programs are inactive (Fang et al., 2013; Gamba et al., 2014; Kikuchi et al., 2011; Lepilina et al., 2006). Our results indicate that the repressive code embedded in regeneration enhancers, adjacent to the activation motifs, might contribute to this rapid deactivation. Moreover, we demonstrate that repression ensures a lack of regenerative factor induction in uninjured hearts. Thus, we provide evidence that regenerative tissues require repression to prevent aberrant gene expression. Our studies provide evidence that coordination of activation and repressive motifs confers regeneration enhancer function to govern spatiotemporal gene expression, which supports heart regeneration (Fig. 7).

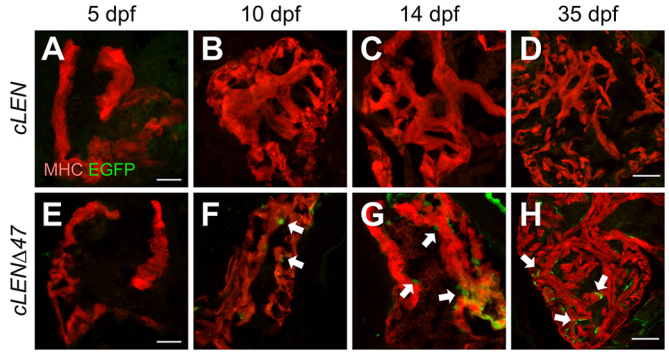

Fig. 6. Developmental emergence of the repression mechanism. Images of sections of the developing hearts of *cLEN* (A-D) and *cLENΔ47* (E-H) reporter fish. Numbers of animals are shown in Table S3. The arrows indicate endocardial EGFP expression. Scale bars: 20 µm in A,E; 50 µm in D,H.

Our results suggest that regulatory elements associated with heart regeneration are subject to repression during cardiac maturation. Similar observations were also reported in the mouse heart. The levels of *insulin-like growth factor 2 mRNA binding protein 3* (*Igf2bp3*), a positive regulator of CM proliferation, are lower in postnatal day 8 matured hearts versus postnatal day 1 immature hearts (Wang et al., 2019). Interestingly, a repressive histone mark and DNA methylation are progressively enriched in the *Igf2bp3* genomic locus during postnatal development, suggesting an emergence of a repressive component during cardiac maturation (Sim et al., 2015; Wang et al., 2019). One approach to promote cardiac regeneration is to revert cardiac maturity from mature to immature states, thereby increasing proliferative ability. Our findings reveal two strategies to achieve this goal, including attenuation of repression and promotion of activation. Triggering activation has been widely attempted, and this approach improves heart regeneration (Cui et al., 2020; Monroe et al., 2019; Tao et al., 2016). However, the impact of mitigating repression on heart regeneration has been little explored. Polycomb repressive complex 2 (PRC2) is the major repressive complex that catalyzes H3K27 trimethylation (H3K27me3) (Cao et al., 2002; Margueron et al., 2009). In mouse hearts, loss of *Ezh1*, a catalytic subunit of PRC2, results in reduced cardiac regeneration, suggesting a positive role of general repressive function in heart regeneration (Ai et al., 2017). In zebrafish hearts, global inhibition of the repressive histone mark H3K27me3 compromises the initiation of heart regeneration owing to the failure of structural gene silencing in the border zone (Ben-Yair et al., 2019). These studies suggest that attenuation of repression might be unable to promote heart regeneration (Ai et al., 2017; Ben-Yair et al., 2019). However, this perturbation might dysregulate vast numbers of genes, which complicates mechanistic interpretations. Further studies are needed to characterize specific repressors regulating regeneration enhancers and to explore whether attenuating repression helps in priming regeneration enhancers and, subsequently, improves heart regeneration.

The impact of repression in the uninjured tissues is a fundamental problem. Previous studies demonstrated that repression plays certain roles in supporting terminal differentiation and safeguarding proper tissue homeostasis (Ma et al., 2015; Sun et al., 2016). Schwann cells and liver constitute regenerative tissues in mammals. Loss of PRC2 in Schwann cells results in upregulation of injury-responsive genes, implying that repression is required for inhibition of aberrant gene expression in the absence of injury. Importantly, Schwann cells lacking PRC2 function display abnormalities of myelin, including morphological changes and progressive hypermyelination (Ma et al., 2015), emphasizing the impact of repression on the function of uninjured tissues. In the mammalian liver, *Arid1a*, a key component of the ATP-dependent chromatin-remodeling complex, plays repressive roles, which contribute to differentiation of the liver after birth (Sun et al., 2016). Although the mutation of *lepb*, a target gene of *LEN*, is unlikely to influence regeneration ability in zebrafish (Kang et al., 2016), it will be interesting to determine whether disruption of the endogenous repressive motif in *cLEN* yields ectopic *lepb* expression in uninjured hearts and, subsequently, influences endocardial function.

Our in-depth investigation of the cardiac regeneration enhancer at the molecular level provides evidence for a new model of regeneration enhancer function. In addition, studies in *Drosophila* imaginal disc demonstrated that the dual-component mechanism in regeneration enhancers influences regenerative capacity (Harris et al., 2016, 2020). It would be interesting to determine whether this

Development (2020) 147, dev194019. doi:10.1242/dev.194019

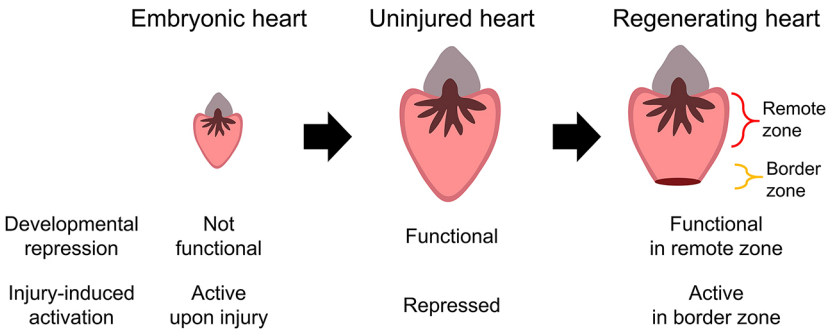

Fig. 7. Proposed model of regulation of the activity of cardiac TREEs in uninjured and regenerating hearts. In uninjured embryonic hearts, cardiac TREEs are inactive; they are activated upon injury. Repression of cardiac TREEs is not functional in the heart in early development. During maturation, cardiac TREEs are actively repressed to prevent aberrant activation in uninjured tissues. Upon injury, the dual function of distinct *cis*-regulatory elements restricts cardiac TREE activation to the wounded area.

dual-component mechanism can be extrapolated to regeneration enhancers operating in diverse cells and tissues as a general phenomenon. The results of this study can be adapted to other contexts to understand the mechanism of regeneration. A comprehensive understanding of transcriptional regulation at the level of regeneration enhancers will allow the construction of the gene regulatory network responsible for tissue regeneration.

MATERIALS AND METHODS

Maintenance of zebrafish and other *Danio* fish species and procedures

Wild-type or transgenic male and female zebrafish of the outbred Ekkwill (EK) strain ranging up to 12 months of age were used for all zebrafish experiments. Wild types of *Danio aesculapii*, *Danio kyathit* and *Danio albolineatus* from 6 to 18 months of age were used for the experiments. The water temperature was maintained at 28°C for animals unless otherwise indicated. Partial ventricular resection surgery was performed as described previously (Poss et al., 2002), in which ∼20% of the cardiac ventricle was removed at the apex. For expression patterns to determine enhancer activity, at least four hearts, unless indicated, were examined per line. To ablate CMs, *cmlc2:mCherry-NTR* fish were used (Chen et al., 2013). To ablate CMs of larvae, juveniles and adults, 3 dpf, 7 wpf and 4 mpf *cmlc2:mCherry-NTR* zebrafish were incubated in 10, 10 and 5 mM metronidazole for 18, 24 and 24 h, respectively. Work with zebrafish and other *Danio* fish species was performed in accordance with University of Wisconsin-Madison guidelines.

To define the activity of various *cLEN* fragments, 26 additional new transgenic lines (listed in Table S2) were established in this study. I-SceI meganuclease transgenesis was used to generate transgenic animals. DNA sequences were amplified by PCR with the indicated primers (Table S1) and subcloned into the pCS2-P2:EGFP-I-SceI vector, in which I-SceI restriction sites were flanked by a multiple cloning site. The 2 kb upstream sequences of *lepb* (*P2*) were used as the minimal promoter. The In-Fusion Cloning technique was used for deletion and insertion of *cLEN* with the corresponding primers (Table S1). The rationale behind the deletion of 11 bp is to remove approximately a single helical turn of the DNA (Bond et al., 2010), potentially allowing for maintenance of the integrity of the chromatin after the deletion. The Q5 site-directed mutagenesis kit (NEB) was used to mutate GTCA to CATT. Both the In-Fusion Cloning technique and the Q5 site-directed mutagenesis kit were used to mutate the AP-1 binding sites. The *AFNEGx3* synthetic enhancer fragment was generated by annealing two complementary single stranded oligonucleotides. These constructs were injected into one-cell-stage wild-type embryos using standard meganuclease transgenesis techniques. To isolate the stable lines, larvae were examined for transgene expression near the injury site in response to fin fold amputation. *P2* induced transgene expression after fin fold amputation at larval stages, but there was no induction after caudal fin amputation in adults (Fig. S1A; Kang et al., 2016).

To generate mRNAs, the *junba*, *fosl1a*, *nfatc1* and *mCherry* open reading frames were cloned downstream of the SP6 promoter in the pCS2-I-SceI vector. mRNA was synthesized using an SP6 mMESSAGE mMachine kit (Ambion) according to the manufacturer's instructions. A total of 60 pg of mRNA (30 pg each of *junba* and *fosl1a* for AP-1 and 20 pg each of *junba*, *fosl1a* and *nfatc1* in AP-1+*nfatc1* co-injection experiments) was injected into wild-type one-cell-stage *cLEN:EGFP* heterozygote embryos. Embryos were collected 1 day post-injection, and gene expression analysis was performed by imaging EGFP and mCherry signals and by RT-qPCR for *EGFP*. Four or five embryos per sample were used to extract the total RNA. Genomic DNA (gDNA) from *D. aesculapii*, *D. kyathit* and *D. albolineatus* was obtained by collecting fins and purifying the genomic DNA using a Gentra Puregene tissue kit (QIAGEN, 158667). *cLEN* orthologous regions from each species were amplified by PCR with gDNA using multiple combinations of forward and reverse primers targeting zebrafish *cLEN*. PCR was performed using Thermotaq DNA Polymerase (NEB, M0267) or Phusion high-fidelity DNA polymerase (NEB, M0530). Forward primers B1, B7, L233 and L246 and reverse primers B8, L193, L231 and L239 successfully amplified *cLEN* in all species (Table S1). Using primer pairs B1-B8, B7-B8, L233-L231 and L246-L239, all or part of *cLEN* in each species was amplified via PCR, and the amplicons were subcloned into pJET1.2/blunt cloning vectors using a CloneJET PCR cloning kit (Thermo Scientific, K1231). Plasmids were sequenced via Sanger sequencing using the primer targeting the T7 promoter (5′-TAATACGACTCACTATAGGG-3′) at Functional Biosciences, Inc. (Madison, WI, USA). Sequencing results were analyzed and aligned to zebrafish *cLEN* using SnapGene (GSL Biotech LLC).

Histology and imaging

Hearts were fixed with 4% paraformaldehyde overnight at 4°C or for 1 h at room temperature. Cryosectioning and immunohistochemistry were performed as described previously, with modifications (Kang et al., 2016). Hearts were cryosectioned at 10 µm thickness. Heart sections were equally distributed onto four or five serial slides such that each slide contained sections representing all areas of the ventricle. A solution comprising 5% goat serum, 1% bovine serum albumin, 1% dimethyl sulfoxide and 0.1% Tween-20 was used for blocking and antibody staining. The primary and secondary antibodies used in this study were as follows: anti-myosin heavy chain (mouse; F59; Developmental Studies Hybridoma Bank; 1:50), anti-EGFP (rabbit; A11122; Life Technologies; 1:200), anti-EGFP (chicken; GFP-1020; Aves Labs; 1:2000), anti-Ds-Red (rabbit; 632496; Clontech; 1:500), anti-Raldh2 (rabbit; GTX124302; Genetex; 1:200), Alexa Fluor 488 (mouse, rabbit and chicken; A11029, A11034 and A11039; Life Technologies; 1:500) and Alexa Fluor 594 (mouse and rabbit; A11032 and A11037; Life Technologies; 1:500). Whole-mount larval images were acquired using an AxioZoom stereofluorescence microscope (Zeiss) at the time points indicated. Images of cardiac tissue sections were acquired using an LSM 700 confocal microscope (Zeiss), Eclipse Ti-U inverted compound microscope (Nikon) or BZ-X810 fluorescence microscope (Keyence). Images were processed using ZEN (Zeiss), BZ-X800 analyzer (Keyence) or FIJI/ImageJ software. Image stitching was automatically processed using a ZEN or BZ-X800 analyzer. Further image processing was carried out manually using Photoshop or FIJI/ImageJ software.

Quantification

Quantification of the EGFP intensity and EGFP$^+$ area was performed using the FIJI/ImageJ software. One to five sections were used to determine the values in one cardiac sample. For quantification of the EGFP intensity

Development (2020) 147, dev194019. doi:10.1242/dev.194019

(Fig. 1H; Fig. S8E), images of sections of wounded or uninjured apical regions were converted to 8 bit and adjusted with the threshold, which was determined by the autofluorescence level of CMs. Red channel (MHC) images were used to guide manual selection of heart outlines, which were saved to the region of interest (ROI) manager, after which values of integrated density in ROIs were measured. The EGFP intensity was calculated by normalizing to the intensity in wild-type uninjured heart samples. To quantify the EGFP intensity in Raldh2$^+$ cells (Fig. S3C), the red channel (Raldh2) images were used to define ROIs, and the values of the integrated density in ROIs were calculated. The averaged EGFP intensity level of the border zone was divided by that of the remote zone in the same heart. To measure the EGFP$^+$ area of uninjured hearts, ROIs were determined by manual selection of heart outlines, with guidance provided by the red channel (MHC) images. A remote zone was selected as a 155 µm×450 µm rectangular section at least 250 µm away from the border zone. To quantify the EGFP$^+$ area, selected ROIs were converted to 8 bit, adjusted with the threshold, which was determined by the autofluorescence level of CMs, and the EGFP$^+$ areas in ROIs were evaluated.

VISTA analysis

Zebrafish genomic sequences from *dre-mir-129-1* through *lepb* were aligned via the VISTA alignment tool (http://genome.lbl.gov/vista/index.shtml) against equivalent sequences in golden-line barbel (*Sinocyclocheilus grahami*), horned golden-line barbel (*Sinocyclocheilus rhinocerous*), blind barbel (*Sinocyclocheilus anshuiensis*), German mirror carp (*Cyprinus carpio carpio*), Songpu mirror carp (*Cyprinus carpio carpio*), Hebao red carp (*Cyprinus carpio wuyuanensis*), Yellow River carp (*Cyprinus carpio haematopterus*), goldfish (*Carassius auratus*), Mexican tetra (*Astyanax mexicanus*), Pachon cavefish (*Astyanax mexicanus*), red-bellied piranha (*Pygocentrus nattereri*), electric eel (*Electrophorus electricus*), Atlantic herring (*Clupea harengus*), denticle herring (*Denticeps clupeoides*) and Japanese medaka (*Oryzias latipes*). The genomic location of each sequence is listed in Table S4. VISTA alignment results for *dre-mir-129-1* though *lepb*, *cLEN*, *cLEN-act* and *cLEN-22* were visualized using the VISTA-Point visualization tool.

RNA isolation and RT-qPCR

RNA was isolated from uninjured and partly resected hearts using Tri-Reagent (ThermoFisher). Complementary DNA (cDNA) was synthesized from 300 ng to 1 µg of total RNA using a NEB ProtoScript II first strand cDNA synthesis kit (NEB, E6560). To design *lepb* qPCR primers for other *Danio* species, we initially ran a PCR on gDNA of each species using multiple combinations of primers targeting zebrafish *lepb*. L71 (forward primer, targets upstream of *lepb* exon 1) and L6 (reverse primer, targets *lepb* intron 1) successfully amplified the first exon of *lepb* in each species (Table S1). The amplicons were purified, subcloned into the pJET1.2/blunt cloning vectors, sequenced and analyzed as described above. Based on conserved sequences across all species, we designed the forward primer B27, which targets exon 1 (Table S1). To design a reverse qPCR primer targeting *lepb* exon 2, we first compared *lepb* exon 2 sequences of zebrafish, Pachon cavefish (*Astyanax mexicanus*), red-bellied piranha (*Pygocentrus nattereri*) and Japanese medaka (*Oryzias latipes*). Based on these analyses, we designed the forward (B23 and B24) and reverse primers (B25 and B6) with degenerated nucleotides at locations that differed across species (Table S1). Each of these degenerated primers amplified *lepb* fragments from gDNA of other *Danio* species. We then amplified *lepb* exon 2 from gDNA in each species (Table S1), and the amplicons were purified, subcloned into pJET1.2/blunt cloning vectors, sequenced and analyzed as described above. Based on conserved sequences across *Danio* species, the reverse primer B28 was designed to target exon 2. We confirmed that the B27 and B28 primers successfully amplified the *lepb* cDNA fragment. Quantitative PCR was performed using the qPCRBIO SyGreen Blue Mix Separate-ROX (Genesee Scientific, 17-507) and a Bio-Rad CFX Connect system. All samples were analyzed in biological triplicate with two technical repeats. The sequences of the primers used are listed in Table S1. *lepb* transcript levels were normalized to *actb2* levels in all experiments.

Acknowledgements

We thank the University of Wisconsin-Madison School of Medicine and Public Health (SMPH) BRMS (Biomedical Research Models Services) staff, Lindsey Tushman and Jonah Mudge, for zebrafish care; Jonah Mudge and Daniel F. McGarry for assistance with sample preparation; and Jingli Cao, Chen-Hui Chen, Deneen M. Wellik and Emery H. Bresnick for comments on the manuscript. We also thank Kenneth Poss for sharing fish lines and for his generous support.

Competing interests

The authors declare no competing or financial interests.

Author contributions

Conceptualization: I.J.B., K.S., F.J.P., J.K.; Methodology: I.J.B., K.S., D.O.-M., A.K., J.K.; Validation: I.J.B., K.S., D.O.-M.; Formal analysis: I.J.B., K.S.; Ivestigation: I.J.B., K.S., D.O.-M., A.K.,J.K.; Resources: I.J.B., K.S., N.L., T.J.C., F.J.P., J.K.; Writing - original draft: I.J.B., J.K.; Writing - review & editing: I.J.B., K.S., D.O.-M., J.K.; Visualization: I.J.B., K.S., D.O.-M., J.K.; Supervision: J.K.; Project administration: I.J.B., K.S., J.K.; Funding acquisition: F.J.P., J.K.

Funding

This work was supported by the National Institutes of Health, under a Ruth L. Kirschstein National Research Service Award from the National Heart, Lung and Blood Institute to the University of Wisconsin-Madison Cardiovascular Research Center (T32 HL 007936 to I.J.B.) and from the National Institute Of General Medical Sciences to the University of Wisconsin-Madison Genetics Graduate Training Program (T32 GM 007133 to T.J.C. and D.O.-M.), by a U.S. Department of Agriculture Hatch grant and the University of Wisconsin-Madison UW2020 Round 6 award to F.J.P., by the National Institutes of Health (R35 GM 137878), by University of Wisconsin-Madison start-up funds (AAC8355, AAC8979, AAC6429 and AAG9756), by an American Heart Association grant (AHA16SDG30020001 to J.K.), and by a University of Wisconsin Carbone Cancer Center Support Grant (P30 CA014520 to J.K.). Deposited in PMC for release after 12 months.

Supplementary information

Supplementary information available online at
https://dev.biologists.org/lookup/doi/10.1242/dev.194019.supplemental

Peer review history

The peer review history is available online at
https://dev.biologists.org/lookup/doi/10.1242/dev.194019.reviewer-comments.pdf

References

Ai, S., Yu, X., Li, Y., Peng, Y., Li, C., Yue, Y., Tao, G., Li, C., Pu, W. T. and He, A. (2017). Divergent requirements for EZH1 in heart development versus regeneration. *Circ. Res.* **121**, 106-112. doi:10.1161/CIRCRESAHA.117.311212

Alfonso-Jaume, M. A., Bergman, M. R., Mahimkar, R., Cheng, S., Jin, Z. Q., Karliner, J. S. and Lovett, D. H. (2006). Cardiac ischemia-reperfusion injury induces matrix metalloproteinase-2 expression through the AP-1 components FosB and JunB. *Am. J. Physiol. Heart Circ. Physiol.* **291**, H1838-H1846. doi:10.1152/ajpheart.00026.2006

Beisaw, A., Kuenne, C., Gunther, S., Dallmann, J., Wu, C. C., Bentsen, M., Looso, M. and Stainier, D. (2020). AP-1 Contributes to chromatin accessibility to promote sarcomere disassembly and cardiomyocyte protrusion during zebrafish heart regeneration. *Circ. Res.* **126**, 1760-1778. doi:10.1161/CIRCRESAHA.119.316167

Ben-Yair, R., Butty, V. L., Busby, M., Qiu, Y., Levine, S. S., Goren, A., Boyer, L. A., Burns, C. G. and Burns, C. E. (2019). H3K27me3-mediated silencing of structural genes is required for zebrafish heart regeneration. *Development* **146**, dev178632. doi:10.1242/dev.178632

Bond, L. M., Peters, J. P., Becker, N. A., Kahn, J. D. and Maher, L. J.III (2010). Gene repression by minimal lac loops in vivo. *Nucleic Acids Res.* **38**, 8072-8082. doi:10.1093/nar/gkq755

Brudno, M., Poliakov, A., Minovitsky, S., Ratnere, I. and Dubchak, I. (2007). Multiple whole genome alignments and novel biomedical applications at the VISTA portal. *Nucleic Acids Res.* **35**, W669-W674. doi:10.1093/nar/gkm279

Cao, J. and Poss, K. D. (2018). The epicardium as a hub for heart regeneration. *Nat. Rev. Cardiol.* **15**, 631-647. doi:10.1038/s41569-018-0046-4

Cao, R., Wang, L., Wang, H., Xia, L., Erdjument-Bromage, H., Tempst, P., Jones, R. S. and Zhang, Y. (2002). Role of histone H3 lysine 27 methylation in Polycomb-group silencing. *Science* **298**, 1039-1043. doi:10.1126/science.1076997

Chen, C.-H., Durand, E., Wang, J., Zon, L. I. and Poss, K. D. (2013). zebraflash transgenic lines for in vivo bioluminescence imaging of stem cells and regeneration in adult zebrafish. *Development* **140**, 4988-4997. doi:10.1242/dev.102053

Cui, M., Wang, Z., Chen, K., Shah, A. M., Tan, W., Duan, L., Sanchez-Ortiz, E., Li, H., Xu, L., Liu, N. et al. (2020). Dynamic transcriptional responses to injury of

regenerative and non-regenerative cardiomyocytes revealed by single-nucleus RNA sequencing. *Dev. Cell* **53**, 102-116.e108. doi:10.1016/j.devcel.2020.02.019
Curado, S., Anderson, R. M., Jungblut, B., Mumm, J., Schroeter, E. and Stainier, D. Y. (2007). Conditional targeted cell ablation in zebrafish: a new tool for regeneration studies. *Dev. Dyn.* **236**, 1025-1035. doi:10.1002/dvdy.21100
Dahl, R., Iyer, S. R., Owens, K. S., Cuylear, D. D. and Simon, M. C. (2007). The transcriptional repressor GFI-1 antagonizes PU.1 activity through protein-protein interaction. *J. Biol. Chem.* **282**, 6473-6483. doi:10.1074/jbc.M607613200
De Val, S. and Black, B. L. (2009). Transcriptional control of endothelial cell development. *Dev. Cell* **16**, 180-195. doi:10.1016/j.devcel.2009.01.014
De Val, S., Chi, N. C., Meadows, S. M., Minovitsky, S., Anderson, J. P., Harris, I. S., Ehlers, M. L., Agarwal, P., Visel, A., Xu, S. M. et al. (2008). Combinatorial regulation of endothelial gene expression by ets and forkhead transcription factors. *Cell* **135**, 1053-1064. doi:10.1016/j.cell.2008.10.049
Fang, Y., Gupta, V., Karra, R., Holdway, J. E., Kikuchi, K. and Poss, K. D. (2013). Translational profiling of cardiomyocytes identifies an early Jak1/Stat3 injury response required for zebrafish heart regeneration. *Proc. Natl. Acad. Sci. USA* **110**, 13416-13421. doi:10.1073/pnas.1309810110
Fukuda, R., Gunawan, F., Ramadass, R., Beisaw, A., Konzer, A., Mullapudi, S. T., Gentile, A., Maischein, H. M., Graumann, J. and Stainier, D. Y. R. (2019). Mechanical forces regulate cardiomyocyte myofilament maturation via the VCL-SSH1-CFL axis. *Dev. Cell* **51**, 62-77.e65. doi:10.1016/j.devcel.2019.08.006
Gabisonia, K., Prosdocimo, G., Aquaro, G. D., Carlucci, L., Zentilin, L., Secco, I., Ali, H., Braga, L., Gorgodze, N., Bernini, F. et al. (2019). MicroRNA therapy stimulates uncontrolled cardiac repair after myocardial infarction in pigs. *Nature* **569**, 418-422. doi:10.1038/s41586-019-1191-6
Gamba, L., Harrison, M. and Lien, C. L. (2014). Cardiac regeneration in model organisms. *Curr. Treat. Options Cardiovasc. Med.* **16**, 288. doi:10.1007/s11936-013-0288-8
Gemberling, M., Karra, R., Dickson, A. L. and Poss, K. D. (2015). Nrg1 is an injury-induced cardiomyocyte mitogen for the endogenous heart regeneration program in zebrafish. *eLife* **4**, e05871. doi:10.7554/eLife.05871.015
Goldman, J. A., Kuzu, G., Lee, N., Karasik, J., Gemberling, M., Foglia, M. J., Karra, R., Dickson, A. L., Sun, F., Tolstorukov, M. Y. et al. (2017). Resolving heart regeneration by replacement histone profiling. *Dev. Cell* **40**, 392-404.e395.doi:10.1016/j.devcel.2017.01.013
Gonzalez-Rosa, J. M., Burns, C. E. and Burns, C. G. (2017). Zebrafish heart regeneration: 15 years of discoveries. *Regeneration (Oxf)* **4**, 105-123. doi:10.1002/reg2.83
Gorissen, M. and Flik, G. (2014). Leptin in teleostean fish, towards the origins of leptin physiology. *J. Chem. Neuroanat.* **61-62**, 200-206. doi:10.1016/j.jchemneu.2014.06.005
Gorissen, M., Bernier, N. J., Nabuurs, S. B., Flik, G. and Huising, M. O. (2009). Two divergent leptin paralogues in zebrafish (Danio rerio) that originate early in teleostean evolution. *J. Endocrinol.* **201**, 329-339. doi:10.1677/JOE-09-0034
Harper, J., Mould, A., Andrews, R. M., Bikoff, E. K. and Robertson, E. J. (2011). The transcriptional repressor Blimp1/Prdm1 regulates postnatal reprogramming of intestinal enterocytes. *Proc. Natl. Acad. Sci. USA* **108**, 10585-10590. doi:10.1073/pnas.1105852108
Harris, R. E., Setiawan, L., Saul, J. and Hariharan, I. K. (2016). Localized epigenetic silencing of a damage-activated WNT enhancer limits regeneration in mature Drosophila imaginal discs. *eLife* **5**, e11588. doi:10.7554/eLife.11588.028
Harris, R. E., Stinchfield, M. J., Nystrom, S. L., McKay, D. J. and Hariharan, I. K. (2020). Damage-responsive, maturity-silenced enhancers regulate multiple genes that direct regeneration in Drosophila. *eLife* **9**, e58305. doi:10.7554/eLife.58305.sa2
Hohenauer, T. and Moore, A. W. (2012). The Prdm family: expanding roles in stem cells and development. *Development* **139**, 2267-2282. doi:10.1242/dev.070110
Huang, W., Zhang, R. and Xu, X. (2009). Myofibrillogenesis in the developing zebrafish heart: a functional study of tnnt2. *Dev. Biol.* **331**, 237-249. doi:10.1016/j.ydbio.2009.04.039
Huang, G. N., Thatcher, J. E., McAnally, J., Kong, Y., Qi, X., Tan, W., DiMaio, J. M., Amatruda, J. F., Gerard, R. D., Hill, J. A. et al. (2012). C/EBP transcription factors mediate epicardial activation during heart development and injury. *Science* **338**, 1599-1603. doi:10.1126/science.1229765
Huising, M. O., Geven, E. J., Kruiswijk, C. P., Nabuurs, S. B., Stolte, E. H., Spanings, F. A., Verburg-van Kemenade, B. M. and Flik, G. (2006). Increased leptin expression in common Carp (Cyprinus carpio) after food intake but not after fasting or feeding to satiation. *Endocrinology* **147**, 5786-5797. doi:10.1210/en.2006-0824
Hung, H. A., Sun, G., Keles, S. and Svaren, J. (2015). Dynamic regulation of Schwann cell enhancers after peripheral nerve injury. *J. Biol. Chem.* **290**, 6937-6950. doi:10.1074/jbc.M114.622878
Ishida, T., Nakajima, T., Kudo, A. and Kawakami, A. (2010). Phosphorylation of Junb family proteins by the Jun N-terminal kinase supports tissue regeneration in zebrafish. *Dev. Biol.* **340**, 468-479. doi:10.1016/j.ydbio.2010.01.036
Kallies, A., Hawkins, E. D., Belz, G. T., Metcalf, D., Hommel, M., Corcoran, L. M., Hodgkin, P. D. and Nutt, S. L. (2006). Transcriptional repressor Blimp-1 is essential for T cell homeostasis and self-tolerance. *Nat. Immunol.* **7**, 466-474. doi:10.1038/ni1321
Kang, J., Hu, J., Karra, R., Dickson, A. L., Tornini, V. A., Nachtrab, G., Gemberling, M., Goldman, J. A., Black, B. L. and Poss, K. D. (2016). Modulation of tissue repair by regeneration enhancer elements. *Nature* **532**, 201-206. doi:10.1038/nature17644
Karra, R., Foglia, M. J., Choi, W.-Y., Belliveau, C., DeBenedittis, P. and Poss, K. D. (2018). Vegfaa instructs cardiac muscle hyperplasia in adult zebrafish. *Proc. Natl. Acad. Sci. USA* **115**, 8805-8810. doi:10.1073/pnas.1722594115
Khan, A., Fornes, O., Stigliani, A., Gheorghe, M., Castro-Mondragon, J. A., van der Lee, R., Bessy, A., Cheneby, J., Kulkarni, S. R., Tan, G. et al. (2018). JASPAR 2018: update of the open-access database of transcription factor binding profiles and its web framework. *Nucleic Acids Res.* **46**, D1284. doi:10.1093/nar/gkx1188
Kikuchi, K., Holdway, J. E., Major, R. J., Blum, N., Dahn, R. D., Begemann, G. and Poss, K. D. (2011). Retinoic acid production by endocardium and epicardium is an injury response essential for zebrafish heart regeneration. *Dev. Cell* **20**, 397-404. doi:10.1016/j.devcel.2011.01.010
Kvon, E. Z. (2015). Using transgenic reporter assays to functionally characterize enhancers in animals. *Genomics* **106**, 185-192. doi:10.1016/j.ygeno.2015.06.007
Lee, H. J., Hou, Y., Chen, Y., Dailey, Z. Z., Riddihough, A., Jang, H. S., Wang, T. and Johnson, S. L. (2020). Regenerating zebrafish fin epigenome is characterized by stable lineage-specific DNA methylation and dynamic chromatin accessibility. *Genome Biol.* **21**, 52. doi:10.1186/s13059-020-1948-0
Lepilina, A., Coon, A. N., Kikuchi, K., Holdway, J. E., Roberts, R. W., Burns, C. G. and Poss, K. D. (2006). A dynamic epicardial injury response supports progenitor cell activity during zebrafish heart regeneration. *Cell* **127**, 607-619. doi:10.1016/j.cell.2006.08.052
Li, H., Ji, M., Klarmann, K. D. and Keller, J. R. (2010). Repression of Id2 expression by Gfi-1 is required for B-cell and myeloid development. *Blood* **116**, 1060-1069. doi:10.1182/blood-2009-11-255075
Ma, K. H., Hung, H. A., Srinivasan, R., Xie, H., Orkin, S. H. and Svaren, J. (2015). Regulation of peripheral nerve myelin maintenance by gene repression through polycomb repressive complex 2. *J. Neurosci.* **35**, 8640-8652. doi:10.1523/JNEUROSCI.2257-14.2015
Margueron, R., Justin, N., Ohno, K., Sharpe, M. L., Son, J., Drury, W. J., III, Voigt, P., Martin, S. R., Taylor, W. R., De Marco, V. et al. (2009). Role of the polycomb protein EED in the propagation of repressive histone marks. *Nature* **461**, 762-767. doi:10.1038/nature08398
Marin-Juez, R., El-Sammak, H., Helker, C. S. M., Kamezaki, A., Mullapuli, S. T., Bibli, S. I., Foglia, M. J., Fleming, I., Poss, K. D. and Stainier, D. Y. R. (2019). Coronary revascularization during heart regeneration is regulated by epicardial and endocardial cues and forms a scaffold for cardiomyocyte repopulation. *Dev. Cell* **51**, 503-515.e504. doi:10.1016/j.devcel.2019.10.019
Meadows, S. M., Myers, C. T. and Krieg, P. A. (2011). Regulation of endothelial cell development by ETS transcription factors. *Semin. Cell Dev. Biol.* **22**, 976-984. doi:10.1016/j.semcdb.2011.09.009
Monroe, T. O., Hill, M. C., Morikawa, Y., Leach, J. P., Heallen, T., Cao, S., Krijger, P. H. L., de Laat, W., Wehrens, X. H. T., Rodney, G. G. et al. (2019). YAP Partially reprograms chromatin accessibility to directly induce adult cardiogenesis In Vivo. *Dev. Cell* **48**, 765-779.e767. doi:10.1016/j.devcel.2019.01.017
Muncan, V., Heijmans, J., Krasinski, S. D., Buller, N. V., Wildenberg, M. E., Meisner, S., Radonjic, M., Stapleton, K. A., Lamers, W. H., Biemond, I. et al. (2011). Blimp1 regulates the transition of neonatal to adult intestinal epithelium. *Nat. Commun.* **2**, 452. doi:10.1038/ncomms1463
Nemer, G. and Nemer, M. (2002). Cooperative interaction between GATA5 and NF-ATc regulates endothelial-endocardial differentiation of cardiogenic cells. *Development* **129**, 4045-4055.
Norrmén, C., Ivanov, K. I., Cheng, J., Zangger, N., Delorenzi, M., Jaquet, M., Miura, N., Puolakkainen, P., Horsley, V., Hu, J. et al. (2009). FOXC2 controls formation and maturation of lymphatic collecting vessels through cooperation with NFATc1. *J. Cell Biol.* **185**, 439-457. doi:10.1083/jcb.200901104
Park, C., Kim, T. M. and Malik, A. B. (2013). Transcriptional regulation of endothelial cell and vascular development. *Circ. Res.* **112**, 1380-1400. doi:10.1161/CIRCRESAHA.113.301078
Poss, K. D., Wilson, L. G. and Keating, M. T. (2002). Heart regeneration in zebrafish. *Science* **298**, 2188-2190. doi:10.1126/science.1077857
Rodriguez, A. M. and Kang, J. (2020). Regeneration enhancers: starting a journey to unravel regulatory events in tissue regeneration. *Semin. Cell Dev. Biol.* **97**, 47-54. doi:10.1016/j.semcdb.2019.04.003
Rottbauer, W., Saurin, A. J., Lickert, H., Shen, X., Burns, C. G., Wo, Z. G., Kemler, R., Kingston, R., Wu, C. and Fishman, M. (2002). Reptin and pontin antagonistically regulate heart growth in zebrafish embryos. *Cell* **111**, 661-672. doi:10.1016/S0092-8674(02)01112-1
Saleque, S., Kim, J., Rooke, H. M. and Orkin, S. H. (2007). Epigenetic regulation of hematopoietic differentiation by Gfi-1 and Gfi-1b is mediated by the cofactors CoREST and LSD1. *Mol. Cell* **27**, 562-572. doi:10.1016/j.molcel.2007.06.039
Shirali, A. S., Romay, M. C., McDonald, A. I., Su, T., Steel, M. E. and Iruela-Arispe, M. L. (2018). A multi-step transcriptional cascade underlies vascular regeneration in vivo. *Sci. Rep.* **8**, 5430. doi:10.1038/s41598-018-23653-3

Shlyueva, D., Stampfel, G. and Stark, A. (2014). Transcriptional enhancers: from properties to genome-wide predictions. *Nat. Rev. Genet.* **15**, 272-286. doi:10.1038/nrg3682

Sim, C. B., Ziemann, M., Kaspi, A., Harikrishnan, K. N., Ooi, J., Khurana, I., Chang, L., Hudson, J. E., El-Osta, A. and Porrello, E. R. (2015). Dynamic changes in the cardiac methylome during postnatal development. *FASEB J.* **29**, 1329-1343. doi:10.1096/fj.14-264093

Soukup, A. A., Zheng, Y., Mehta, C., Wu, J., Liu, P., Cao, M., Hofmann, I., Zhou, Y., Zhang, J., Johnson, K. D. et al. (2019). Single-nucleotide human disease mutation inactivates a blood-regenerative GATA2 enhancer. *J. Clin. Invest.* **129**, 1180-1192. doi:10.1172/JCI122694

Spitz, F. and Furlong, E. E. M. (2012). Transcription factors: from enhancer binding to developmental control. *Nat. Rev. Genet.* **13**, 613-626. doi:10.1038/nrg3207

Sun, X., Chuang, J.-C., Kanchwala, M., Wu, L., Celen, C., Li, L., Liang, H., Zhang, S., Maples, T., Nguyen, L. H. et al. (2016). Suppression of the SWI/SNF component Arid1a promotes mammalian regeneration. *Cell Stem Cell* **18**, 456-466. doi:10.1016/j.stem.2016.03.001

Suzuki, N., Hirano, K., Ogino, H. and Ochi, H. (2019). Arid3a regulates nephric tubule regeneration via evolutionarily conserved regeneration signal-response enhancers. *eLife* **8**, e43186. doi:10.7554/eLife.43186

Tao, G., Kahr, P. C., Morikawa, Y., Zhang, M., Rahmani, M., Heallen, T. R., Li, L., Sun, Z., Olson, E. N., Amendt, B. A. et al. (2016). Pitx2 promotes heart repair by activating the antioxidant response after cardiac injury. *Nature* **534**, 119-123. doi:10.1038/nature17959

Thompson, J. D., Ou, J., Lee, N., Shin, K., Cigliola, V., Song, L., Crawford, G. E., Kang, J. and Poss, K. D. (2020). Identification and requirements of enhancers that direct gene expression during zebrafish fin regeneration. *Development* **147**, dev191262. doi:10.1242/dev.191262

Tzahor, E. and Poss, K. D. (2017). Cardiac regeneration strategies: Staying young at heart. *Science* **356**, 1035-1039. doi:10.1126/science.aam5894

Vizcaya-Molina, E., Klein, C. C., Serras, F., Mishra, R. K., Guigo, R. and Corominas, M. (2018). Damage-responsive elements in Drosophila regeneration. *Genome Res.* **28**, 1852-1866. doi:10.1101/gr.233098.117

Wang, Z., Cui, M., Shah, A. M., Ye, W., Tan, W., Min, Y. L., Botten, G. A., Shelton, J. M., Liu, N., Bassel-Duby, R. et al. (2019). Mechanistic basis of neonatal heart regeneration revealed by transcriptome and histone modification profiling. *Proc. Natl. Acad. Sci. USA* **116**, 18455-18465. doi:10.1073/pnas.1905824116

Wang, W., Hu, C. K., Zeng, A., Alegre, D., Hu, D., Gotting, K., Ortega Granillo, A., Wang, Y., Robb, S., Schnittker, R. et al. (2020). Changes in regeneration-responsive enhancers shape regenerative capacities in vertebrates. *Science* **369**, eaaz3090. doi:10.1126/science.aaz3090

Yates, S. and Rayner, T. E. (2002). Transcription factor activation in response to cutaneous injury: role of AP-1 in reepithelialization. *Wound Repair. Regen.* **10**, 5-15. doi:10.1046/j.1524-475X.2002.10902.x

Zhou, B., Wu, B., Tompkins, K. L., Boyer, K. L., Grindley, J. C. and Baldwin, H. S. (2005). Characterization of Nfatc1 regulation identifies an enhancer required for gene expression that is specific to pro-valve endocardial cells in the developing heart. *Development* **132**, 1137-1146. doi:10.1242/dev.01640